66th Meeting of the AEROBALLISTIC RANGE ASSOCIATION
San Antonio, Texas, October 4 - 9, 2015.

# Use of a Tantalum Liner to Reduce Bore Erosion and Increase Muzzle Velocity in Two-Stage Light Gas Guns.

D. W. Bogdanoff

Analytical Mechanics Associates, Inc.
NASA Ames Research Center
Moffett Field, CA 94035-1000

## ABSTRACT

Muzzle velocities and gun erosion predicted by earlier numerical simulations of two stage light gas guns with steel gun tubes were in good agreement with experimental values. In a subsequent study, simulations of high performance shots were repeated with rhenium (Re) gun tubes. Large increases in muzzle velocity (2 - 4 km/sec) were predicted for Re tubes. In addition, the hydrogen-produced gun tube erosion was, in general, predicted to be zero with Re tubes. Tantalum (Ta) has some mechanical properties superior to those of Re. Tantalum has a lower modulus of elasticity than Re for better force transmission from the refractory metal liner to an underlying thick wall steel tube. Tantalum also has greater ductility than Re for better survivability during severe stress/strain cycles. Also, tantalum has been used as a coating or liner in military powder guns with encouraging results. Tantalum has, however, somewhat inferior thermal properties to those of rhenium, with a lower melting point and lower density and thermal conductivity. The present study was undertaken to see to what degree the muzzle velocity gains of rhenium gun tubes (over steel tubes) could be achieved with tantalum gun tubes. Nine high performance shots were modeled with a new version of our CFD gun code for steel, rhenium and tantalum gun tubes. For all except the highest velocity shot, the results with Ta tubes were nearly identical with those for Re tubes. Even for the highest velocity shot, the muzzle velocity gain over a steel tube using Ta was 82% of the gain obtained using Re. Thus, the somewhat inferior thermal properties of Ta (when compared to those of Re) translate into only very slightly poorer overall muzzle velocity performance. When this fact is combined with the superior mechanical properties of Ta and the encouraging performance of Ta liners/coatings in military powder guns, tantalum is to be preferred over Re as a liner/coating material for two stage light gas guns to increase muzzle velocity and reduce bore erosion.

## I. INTRODUCTION

1

The NASA Ames 0.5” two-stage light gas gun is shown (not to scale) in Fig. 1. The operation of such a gun starts with the burning of the powder in the powder chamber. The piston, typically an easily deformable plastic such as polyethylene, is accelerated in the pump tube to velocities of the order of 0.8 km/sec. The hydrogen in front of the piston is greatly compressed and heated by the piston, reaching pressures of the order of 7000 bar and temperatures that are ideally as high as 3000 K. At some point in the compression cycle, the diaphragm just behind the projectile breaks and the projectile begins to

accelerate down the barrel. The highly compressed and heated hydrogen between the piston and the projectile can have a sound speed of ~4 km/sec and can accelerate the projectile to velocities of 7 - 8 km/sec. With very light projectiles and by driving the gun hard (that is, by using large powder loads and/or low hydrogen pump tube fill pressures), velocities up to 11 km/sec can be obtained. Further discussion of two-stage light gas guns is given in Ref. 1.

Gun bore erosion is a serious problem with two-stage light gas guns.[1-3] Excessive gun tube erosion can lead to poor or failed launches due to damage or destruction of the launch package. It can also lead to frequent barrel changes, especially at higher launch velocities, with the corresponding down time. Gun tube erosion can also limit the maximum velocity obtainable by loading down the hydrogen working gas with heavy eroded gun tube material.[3,4] (For brevity, we will use the term "hydrogen loading" to refer to this effect in the remainder of this paper.) One way to mitigate this problem is to perform a series of CFD calculations at various gun operating conditions and then, from this series, to choose optimum sets of gun operating conditions.[5-9] Conditions judged from the calculations to be likely to result in reduced gun erosion can then be tested in actual gun firings. This procedure has been used in earlier work on the 1.5" and 0.5" guns at the NASA Ames Research Center.[7-9]

Gun bore erosion was not directly calculated in the CFD calculations of Refs. 5 - 9, but rough estimates could be made from the calculated values of hydrogen temperature, pressure, velocity and the duration of the erosive conditions. Reference 3 presented a new CFD code in which the bore erosion is directly calculated and the resulting interaction of the eroded material and the hydrogen working gas is modeled. To obtain the erosion rate of the gun bore wall, the unsteady heat conduction into the gun bore wall was solved concurrently with the flow of the various media within the bore. The temperature dependence of the conductivity and specific heat and the phase changes in the gun barrel material were modeled. Mass flux and heat flux at the wall surface were matched between the in-bore media and the gun tube material. The effects of wall mass transfer on friction and the heat transfer were modeled.

In Sec. II, a previously developed CFD light gas gun code is briefly described. We then describe the additions made to the code to allow it to model wall erosion. The first version of the modified code was used to model erosion of steel gun tubes.[3]

In Sec. III, we discuss the selection of new materials for the gun tubes. Tungsten, rhenium, tantalum and a tantalum alloy are considered. Rhenium was selected for the study of Ref. 10. The present study is for tantalum gun tubes. We then describe the changes made to the gun tube material database to allow the code to model refractory metal gun tubes.

In Sec. IV, we review the results obtained in Ref. 3 for operation with steel gun barrels. Therein, CFD results were compared with experimental piston velocity, powder pressure, muzzle velocity and gun erosion data. The experimental data were taken with three different pump tube volumes and included a number of very high velocity launches (up to 9.5 km/sec). The substantial loss of muzzle velocity due to the loading of the hydrogen working gas by the eroded wall material was clearly demonstrated by the experimental and numerical results. Agreement between the CFD calculations which included incorporation of the eroded wall material into the working gas and the experimental data was found to be very good.

The work of Ref. 3 included "normal" modeling, in which the eroded gun tube material is incorporated into the in-bore media and "special" runs, in which all friction, heat transfer and erosion were modeled, but after erosion, the eroded gun tube material is assumed to vanish, rather than to be incorporated into the in-bore media. The special runs are, of course, physically unrealistic. These special runs predicted muzzle velocities up to 2 - 4 km/sec above those of the normal runs for high-performance gun operating conditions. It was then decided to see what fraction of the performance increases predicted by the special runs could be realized using realistic calculations (i.e., calculations with

hydrogen loading), but replacing the gun steel of the gun tubes with rhenium[10] or tantalum (for the present study).

In Sec. V, we present the results of Ref. 10 obtained with rhenium gun tubes. It is shown that the very large increases in muzzle velocity referred to in the previous paragraph are, in fact, predicted to be obtainable using rhenium gun tubes. For almost all the runs modeled, the bore erosion due to heating from the hydrogen working gas is predicted to be zero, because the melting temperature of the rhenium is never reached in the hydrogen zones during the gun cycle. Results are compared for steel and rhenium gun tubes. These results include maximum gun tube surface temperatures and profiles of hydrogen loading with eroded wall material and in-barrel pressures.

In Sec. VI, we present new results for steel, rhenium and tantalum gun tubes. Code modifications and code checks are discussed. Muzzle velocities for the three types of gun tube material are presented. Correlations of total gun tube mass loss versus muzzle velocity and the ratio (powder mass)/(hydrogen mass) are presented. Profiles of tube wall retreat and mass loss along the gun tube are presented and discussed. The overall picture of the new results is presented, along with a discussion of the suitability of tantalum as a gun tube liner/coating material.

In Sec. VII, we discuss scaling of the results obtained with gun size and practical details of the implementation of the refractory metal gun tube technique. This includes length of barrel to be lined with a refractory metal, lining of the gun tube up range of the diaphragm with a refractory metal, and the use of a refractory metal coated diaphragm.

## II. COMPUTATIONAL APPROACH

### A. Original code

The starting point for the CFD code used herein is an earlier CFD code described in Ref. 11. The code models the entire gun firing cycle from gunpowder ignition to the moment that the projectile exits the muzzle. The code is based on the Godunov method in one dimension (solving the Euler equations) and is third-order accurate in space and second order accurate in time. The code is quasi-one-dimensional in that the area of the gun tube varies along the gun. Realistic equations of state are used for all media. The code includes modeling of friction and heat transfer for powder gas, hydrogen, the pump tube piston and the projectile. The frictional and heat transfer terms are added as source terms in the Euler equations. Code validation consisted of comparing CFD results with various analytical solutions and by comparing CFD predictions against experimental data from the Ames 0.5” and 1.5” two-stage light gas guns. In Ref. 9, a grid refinement study was made. Further details regarding the original code can be found in Ref. 10.

### B. Code modifications to allow erosion of gun steel tubes to be modeled

The code modifications are described in Ref. 3 and, in detail, in Ref. 12. Therefore, only a brief outline of the modifications is given below. 3

To perform the calculations required, it is first necessary to obtain the thermal conductivity, specific heat and density of the gun barrel material (gun steel or carbon steel). The heat of the phase changes and the heat of fusion of the steel are also needed. A number of references were consulted and a database of steel properties was compiled. A two-phase equation-of-state (EOS) for the hydrogen-steel mixture was constructed by combining the steel property data with the previously available hydrogen EOS.

The radial heat conduction analysis within the gun bore wall is done in the conventional way. The wall is divided into a number of cells in the axial and radial direction. For the NASA Ames 0.5" light gas gun, there are 200 to 400 cells in the axial direction and 16 cells in the radial direction. The cells are thinnest at the tube bore and increase in thickness as one moves outwards. The total radial thickness of the zone in which the heat conduction is analyzed is 0.042 cm. When the wall temperature exceeds the melting point, material begins to be lost from the wall. To determine the rate at which the wall material is lost, for each time-step, a heat balance is made for the first cell at the gun tube wall.

The method of calculating the barrel wall heat flux in the media in the bore starts with the basic equations[12] for the skin friction and wall heat flux without mass addition (ablation of steel) at the gun tube bore surface. Then, the wall heat flux is corrected[13] (reduced) to allow for the effect of wall mass addition. This mass addition analysis was derived assuming that the medium injected at the wall is the same as the free-stream medium. Since, for our calculations, this is not the case, a further correction[14-16] is added, based on an experimental database, to allow for the difference between the effective molecular weight of the medium injected at the wall and the free-stream medium. Finally, a last correction[12] to the effective molecular weight of the free-stream medium is added, since the free stream is, in general a mixture of hydrogen and steel.

Three quantities must be exchanged between the two parts of the solution, the bore surface temperature and the bore surface heat and mass fluxes. After the mass flux of steel from the barrel bore is calculated for a given cell in the in-bore medium for a given time-step, the state variables of that cell are updated for the addition of steel using the conservation equations.

The present model is incapable of modeling the deposition of steel from the hydrogen-steel mixture back onto the bore surface. In the present model, there is no modeling of incorporation of steel melted off the barrel wall into either the gunpowder/powder gas mixture or the plastic piston. It can be shown that the loss of wall material in these two bore media zones is negligible. Further details of the code modifications are given in Refs. 3 and 12.

## III. SELECTION OF NEW TUBE MATERIAL, DATABASE MODIFICATION

### A. Choice of tube wall materials.

In Ref. 10, rhenium liners for two stage light gas guns were studied. In that reference (pp. 13-14) , the following statements were made. "Ta and Mo were judged to be significantly inferior to Re based on thermal properties and yield strength. Thus, Re is the material of choice for gun tubes." Based on other considerations not taken into account when Ref. 10 was written, these statements must now be regarded as incorrect. The metals with the highest melting points are rhenium (Re), tantalum (Ta) and tungsten (W). Table 1 gives relevant properties of these metals plus those of a Ta – 10% W alloy which has been used as a gun barrel liner. Also given are data for gun steel. The data of Table 10 were taken from Refs. 17 – 19 and the material property values are at room temperature. The refractory metals are very expensive and therefore must be used as liners or coatings in gun tubes, with the main material of the gun tube usually being gun steel. In Ref. 20, the effect of the elastic modulus of the liner/coating materials is discussed. It is pointed out that those liner/coating materials with moduli greater than that of the gun steel jacket do not effectively transfer the load to the jacket material and are prone to cracking. By contrast, those liner/coating materials with moduli less than that of the jacket, especially if they are ductile, effectively transfer the load to the jacket and are not prone to cracking.

**Table 1. Key properties of potential materials for gun barrel liners or coatings.**

| Metal | Re | Ta | Ta-10W | W | Gun steel |
|---|---|---|---|---|---|
| Modulus of elasticity, Msi | 68 | 27 | 29 | 59 | 30 |
| Tensile strength, ksi | 280 | 60 | 160 | 220 | |
| Reduction of area, % | 35 | 95+ | 85+ | 0 | |
| Melting point, K | 3456 | 3269 | 3320 | 3683 | 1723 |
| Density, g/cm$^3$ | 21 | 16.6 | | 19.2 | 7.8 |
| Thermal conductivity, W/m/K | 75.6 | 54.5 | | 167.1 | 43 |
| Specific heat, kJ/kg/K | 0.147 | 0.151 | | 0.142 | 0.473 |

Tantalum and Ta-10W and similar alloys have been used as liners and coatings in military powder guns and have been shown to be effective in reducing gun barrel erosion. Reference 21 discusses the use Ta-10W and T222 alloy (Ta-10W-2.5Hf-0.01C) liners in a 7.62 mm gun system to reduce erosion. (Other liner materials were also discussed in Ref. 21.) References 22 – 24 discuss the use of tantalum coatings over steel in a 20 mm gun system and very encouraging results were obtained. From Table 1, it is seen that the thermal properties of tantalum are somewhat inferior to those of rhenium, in that the melting point, density and thermal conductivity of tantalum are lower than the corresponding values for rhenium. However, the increase in melting point of Ta over gun steel is nearly 90% of the increase available with rhenium. Based on the discussion of the preceding paragraph and the successful implementation of tantalum and tantalum alloy liners/coatings discussed in Refs. 22 – 24, it is apparent that tantalum is a strong candidate for the liner/coating for a two-stage light gas gun. Tantalum liners/coatings are the main subject of the present report.

It has been suggested to use refractory ceramic materials (carbides, etc.) as gun tube liners instead of refractory metals. However, such materials, on account of their brittleness, are very likely to crack and shatter in the severe thermal and pressure environment of the gun tubes and therefore, they are not likely to be suitable for such service.

**B. Data base modifications to allow erosion of refractory metal tubes to be modeled**

The code, itself, required no significant changes to allow refractory metal gun tubes to be modeled. It was only necessary to construct databases for the refractory metals for the code. Thermal conductivity, specific heat and thermal expansion (density) data for rhenium were obtained from Refs. 25 - 27, respectively. The heat of fusion of rhenium was obtained from Ref. 28. Densities of various solid and liquid metals (Fe, Pd, Pt and Au) were obtained from Refs. 29 and 30, respectively. The ratios of the liquid densities at the melting point to the solid densities at room temperature were calculated and the average value of this ratio was used to estimate a density of liquid rhenium at the melting point. For tantalum, thermal conductivity data was obtained from Ref. 31, specific heat data was obtained from Refs. 32 and 33 (equation) and thermal expansion (density) data was obtained from Ref. 34. The heat of fusion for tantalum was obtained from Ref. 35 and the density of liquid tantalum was obtained from Ref. 36. The volume change and heat of transformation at the melting point were taken into account in constructing the databases. Two-phase equation-of-states (EOS) for hydrogen-rhenium and hydrogen-tantalum mixtures were constructed in the same way as was done for the hydrogen-steel mixture (see Sec. II.B).

## IV. GUN AND CONDITIONS MODELLED; RESULTS WITH STEEL GUN TUBES

### A. Gun and conditions modeled

Figure 1 shows a schematic sketch of one of the modeling configurations of the Ames 0.5" light gas gun. The numbers (in cm) are either the bore diameters or the distances from the blind end of the powder chamber. WG1 - WG4 denote the whisker gauges used to measure piston velocity. In the calculations, the diaphragm is treated as a closed end boundary condition until the pressure at the diaphragm first exceeds the diaphragm rupture pressure; at that point the diaphragm is instantly removed. Table 2 shows the four blocks of data (45 shots total) which were modeled in the studies of Refs. 3 and 12. The powder types are the IMR/DuPont designations of the powder. The break valve (diaphragm) rupture pressures are given in kilobars. The piston velocities are those measured between whisker gauges 2 and 3. Also given are the nominal pump tube volumes and the contraction cone angles. The contraction cone is the conical section which joins the pump tube and the barrel. (The contraction cone angles given herein are always the full angle, not the half angles.) There are four blocks of data, separated by the vertical lines, in Table 2. Type 4198 powder was used for data block 1 and type 4895 powder for the remaining data blocks. The nominal pump tube volumes are 100% for the first two data blocks and 60% and 40% for data blocks 3 and 4, respectively. There are also differences in the contraction cone angles between the data blocks, as shown in Table 2; these are believed to be less important than the differences in the powder types and the pump tube volumes. The configurations of the gun for the various data blocks are as follows:

Data block 1: Dimensions as shown in Fig. 1.
Data block 2: Cone angle changed to 8.1 deg.
Data block 3: All axial dimensions to the right of WG1 reduced by 607.22 cm; cone angle changed to 8.1 deg.
Data block 4: All axial dimensions to the right of WG1 reduced by 911.82 cm; cone angle changed to 8.1 deg. for part of data block.

For data in blocks 2, 3 and 4 with the 8.1 degree cone angle, the axial dimension at the large end of the cone was shifted to accommodate this cone angle.

**Table 2. Ames 0.5" gun operating conditions for the blocks of data modelled.**

| Data block | 1 | 2 | 3 | 4 |
|---|---|---|---|---|
| No. of shots | 17 | 4 | 9 | 15 |
| Shots modelled, steel, l | 17 | 4 | 9 | 15 |
| Shots modelled, steel, no l | 17 | 3 | 7 | 9 |
| Shots modelled, Re, l | 9 | 0 | 3 | 5 |
| Shots modelled, Ta, l | 9 | 0 | 0 | 0 |
| Launch mass (gms) | 0.88 - 3.17 | 1.17 - 1.41 | 1.16 - 1.44 | 1.07 - 1.41 |
| Powder mass (gms) | 150 - 275 | 187 - 195 | 175 - 197 | 170 - 219 |
| Piston mass (gms) | 888 - 1115 | 819 - 821 | 707 - 720 | 710 - 720 |
| Powder type | 4198 | 4895 | 4895 | 4895 |
| Hydrogen pressure (bar) | 0.69 - 2.07 | 1.32 - 2.07 | 1.70 - 3.39 | 2.60 - 4.06 |
| Break valve pressure (kbar) | 0.69 - 1.38 | 0.29 | 0.29 - 0.31 | 0.31 |
| Piston velocity (m/sec) | 728 - 981 | 768 - 794 | 710 - 823 | 642 - 748 |
| Projectile velocity (km/sec) | 4.97 - 9.46 | 6.24 - 7.30 | 5.62 - 8.06 | 6.71 - 8.08 |
| Pump tube volume | 100% | 100% | 60% | 40% |
| Contract. cone angle (deg) | 12.5 | 8.1 | 8.1 | 8.1, 12.5 |

In the second to sixth lines of Table 3, we see how many of the shots were modeled in different ways. All 45 shots were modeled with steel gun tubes and with loading of the hydrogen with the steel (noted as "steel, l" in the table). Thirty-six of the shots were then modeled with steel gun tubes and no loading of the hydrogen with the steel (noted as "steel, no l" in the table). The results of these two sets of calculations were presented previously in Refs. 3 and 12. In reference 10, seventeen of the shots were re-modeled with rhenium gun tubes with loading of the hydrogen with rhenium (noted as "Re, l" in the table). The shots selected for modeling with rhenium gun tubes were mostly those made with high performance gun operating conditions, where the muzzle velocity gain on shifting from steel to rhenium gun tubes was expected to be the highest. Finally, in the present study, nine of the highest performance shots were re-modeled with tantalum gun tubes with loading of the hydrogen with tantalum (noted as "Ta, l" in the table). Since some changes in the code (notably, an increase in the number of cells in the in-tube media and for the tube walls) had been made between the study of Ref. 10 and the present paper, these nine high performance shots were also re-modeled with steel and rhenium gun tubes with the modified version of the code. (At a later point, it will be shown that results with the new version of the code differ very little from the earlier results.)

**B. Earlier results with steel gun tubes, code validation**

As these results for steel gun tubes were presented in detail in Refs. 3 and 12, here we give only a brief summary. Agreement between the experimental and numerically calculated piston velocities was excellent (±2%) for data blocks 1 and 2. For the same shots, the agreement of the maximum powder pressures was very good (±10%). The errors for data blocks 3 and 4 were about 3 times larger, but still reasonably good for the piston velocity. The greater errors for data blocks 3 and 4 were attributed to much wider variations in the performance of the igniters for the powder charge of the gun for these data blocks.

Experimentally measured gun erosion values were, in many cases, within ±20% to ±40% of the CFD calculated values with maximum differences being mostly less than a factor of two. Overall, we believe that this agreement is reasonably good, considering the complexity of the processes modeled and the fact that the erosion calculations were not tuned in any way.

Figure 2 shows plots of experimental versus numerically calculated muzzle velocity values for data blocks 1 and 2 of Table 1. The uncertainties in the experimental muzzle velocities are estimated to be ±0.3%. Most of the experimental muzzle velocities have been plotted versus two different numerical (CFD) muzzle velocities. For the circle and square data points, the numerical muzzle velocity was calculated with the complete CFD solution, allowing for the loading of the hydrogen gas with the steel ablated from the barrel wall. For the cross data points, the CFD solution has the full frictional and heat transfer losses from the hydrogen to the barrel wall, including the heat losses necessary to ablate the steel from the wall. However, the steel, after being ablated (melted) off the wall, was assumed to disappear. Thus, the difference between the circle and square and the cross data points represents the effect of the loading down of the hydrogen by the steel ablated from the barrel wall. For the shot at the highest velocity, there is no actual experimental muzzle velocity data. For this case the “experimental muzzle velocity” shown in the figure was estimated by scaling from the next lower velocity data point or group of data points. In Fig. 2, the heavy solid line is the line of perfect agreement between experimental and numerical muzzle velocities.

The comparisons made in Fig. 2 cover a wide range of gun operating parameters listed in Table 1 for data blocks 1 and 2. Over this range of parameters, the agreement between the experimental muzzle

velocities and the numerical velocities calculated including loading of the hydrogen by the ablated steel is quite good. Overall, about 2/3 of the muzzle velocities agree within 0.5 km/sec and the worst disagreements are about 0.7 km/sec. At the higher velocities, there are large disagreements between the experimental muzzle velocities and the numerically predicted muzzle velocities calculated without loading of the hydrogen. These disagreements can be as much as 3 to 4 km/sec. The higher muzzle velocities cannot be properly predicted without taking into account the loading of the hydrogen by the ablated barrel wall material.

In Refs. 3 and 12, for data blocks 3 and 4, with loading of the hydrogen, it is shown that agreement between the experimental and numerical muzzle velocities is about the same as that quoted above for data blocks 1 and 2. All of the comparisons of Refs. 3 and 12 are for the Ames 0.5" gun. Code results for modeling the Ames 1.5" and 0.28" guns (Refs. 7 and 37, respectively) at muzzle velocities of ~7 km/s show agreement between experimental and numerical muzzle velocities mostly within 0.2 km/sec, with the largest disagreement being 0.4 km/sec. Code results for the Ames 0.22"/1.28" gun and the GM 0.22"/1.00" gun at muzzle velocities of 10 - 11 km/s also show good agreement between experimental and numerical muzzle velocities with the largest disagreement being 0.6 km/sec. (The experimental data for these guns is given in Ref. 38.) Thus, the code has been well validated for a number of guns and for muzzle velocities ranging from 5 to 11 km/s.

## V. RESULTS WITH RHENIUM GUN TUBES

Results with rhenium tubes are discussed in detail in Ref. 10. Those results are summarized briefly below. For steel gun tubes, the numerical muzzle velocities shown in Fig. 2 which were calculated without hydrogen loading show velocity increases up to 2 - 4 km/sec above those calculated with hydrogen loading. In the study of Ref. 10, we investigated what fraction of the performance increases predicted by the (unrealistic) runs with steel gun tubes without hydrogen loading could be realized by using rhenium gun tubes. To this end, 9 high performance shots modeled in Fig. 2 were re-modeled with realistic calculations (i.e., calculations with hydrogen loading), but replacing the steel of the gun tubes with rhenium. The results of these calculations are shown in Fig. 3. In this figure the cross data points are the same points shown in Fig. 2, for steel tubes without hydrogen loading. The triangle data points are for rhenium tubes with hydrogen loading. (The circle and square data points shown in Fig. 2 for steel tubes with hydrogen loading are not shown in Fig. 3 in the interests of clarity. However, the trend line of perfect agreement between experimental and numerical results has been kept to provide a reference benchmark.) One may see that, except for the highest velocity data point, the numerical muzzle velocities for rhenium tubes with hydrogen loading are very close (within 0.2 km/sec) to the corresponding values for steel tubes without hydrogen loading. Thus, the muzzle velocity gains of 2 - 4 km/sec shown are predicted to actually be realizable using rhenium gun tubes. Similar results were obtained for data blocks 3 and 4. Further analyses of Ref. 10 are summarized below.

Steel gun tubes are predicted to reach their melting point over a substantial length of gun tube (~200 cm) and to have wall retreats of 0.001 - 0.007 cm over these lengths. By contrast, rhenium gun tubes are predicted to reach their melting point over only very short tube lengths (~30 cm) or not at all. For steel gun tubes, large hollows are noted in plots of hydrogen mass fraction versus distance along the gun barrel, reflecting the erosion and inclusion in the working gas of large quantities of the ablated steel gun wall material. At the bottom of the hollows, the mass fraction of hydrogen can drop to as low as 0.25. Plots of density versus distance along the gun barrel show corresponding "humps" where the large quantities of eroded steel are incorporated into the working gas. These "humps" are notably absent in density-distance plots for rhenium tubes. Steep drops in pressure are seen up range of the density

"humps". Much of the pressure force is used to accelerate the heavy ablated steel, leaving much less pressure force available to accelerate the projectile. These steep pressure drops are absent in plots for rhenium tubes. For much of the barrel length, the base pressures with rhenium tubes are calculated to be 1.5 to 1.8 times those for steel tubes. With steel tubes, the heavy hydrogen loading and corresponding reduction in driving pressure available to accelerate the projectile translates in a reduction in the calculated muzzle velocity from 10.00 km/s with rhenium tubes to 8.20 km/s with steel tubes. The latter velocity is in good agreement with the experimental muzzle velocity of 8.08 km/s.

## VI. NEW RESULTS WITH TANTALUM, RHENIUM AND STEEL GUN TUBES

### A. Code modifications and checks

Some code modifications were made between the work of Ref. 10 and the present report. The number of cells in the working media zones were increased. In the older version of the code, the cell counts were mostly 16, 16, 40 (with few being 16, 16, 54). The first number is the cell count in the powder/powder gas zone, the second number is the cell count in the piston plastic zone and the last number is the cell count in the hydrogen/ablated metal zone. Note that there are ghost cells on either end of each zone, so that for nominal cell count of 16, 16, 40, there actually is a cell count of 14, 14, 38 working internal cells. (The ghost cells are used to evaluate the boundary conditions.) The cell count for the working media in the new version of the code is 32, 32, 80. The number of tube wall cells in the axial direction was increased from 200 in the older version of the code to 400 in the present version. The piston friction was re-tuned using a high velocity shot of the Ames 0.5" gun. The present friction values are 0.82 times the values used earlier.

For the present study, numerical calculations with the new version of the code were made for the nine high performance shots seen in Fig. 3 which were modeled for rhenium gun tubes in Ref. 10. To compare apples to apples in the present study, these calculations were made with the new version of the code for steel, rhenium and tantalum tubes. Before embarking on this survey, the differences between results for the older version and the current version were studied for steel gun tubes. Figure 4 shows the comparison of CFD muzzle velocities for nine high performance shots of data block 1 for steel tubes with hydrogen loading. For six of the nine data points, the muzzle velocity differences are less than 0.1 km/s, with the largest difference being 0.18 km/s. Figure 5 shows the same two sets of CFD muzzle velocities plotted versus the experimental muzzle velocities. It is seen that experimental-CFD comparisons are very similar for the two sets of CFD values. It is concluded that the older and current versions of the code give practically the same results. All further results discussed in the following sections were obtained with the current version of the code, with hydrogen loading and are for the gun operating conditions of the nine high performance shots modeled for rhenium tubes seen in Fig. 3.

### B. Muzzle velocities

Figure 6 shows the CFD muzzle velocities for steel, rhenium and tantalum tubes plotted versus the experimental muzzle velocities for steel tubes. It is seen that for seven of the nine shots, the results for tantalum and rhenium tubes are indistinguishable. For the second highest velocity shot, the tantalum tube muzzle velocity is very slightly (~0.040 km/s) less than the rhenium tube muzzle velocity. For the highest velocity shot, the muzzle velocity with tantalum tubes is ~0.70 km/s less than that for rhenium tubes, but even so, the tantalum tubes produce about 82% of the muzzle velocity gain over steel tubes

that can be obtained with rhenium tubes. It is concluded that, overall, tantalum gun tubes can produce a very large fraction of the muzzle velocity gains obtainable with rhenium tubes.

### C. Correlation of total gun tube mass losses

Figure 7 shows the CFD gun tube mass losses for steel, rhenium and tantalum tubes plotted versus the CFD muzzle velocities for steel tubes. Figure 8 shows the same CFD gun tube mass losses plotted versus the ratio (powder mass)/(hydrogen mass). The correlation is somewhat better for Fig. 8 than for Fig. 7, but neither correlation is very tight. This is to be expected, since a number of variables are different among the various shots. This includes the masses of the powder, the piston and the projectile as well as the hydrogen fill pressure and the break valve rupture pressure. With the exception of the highest velocity data point, masses loss for tantalum tubes are 0 to ~0.14 times those for steel tubes and those for rhenium tubes are 0 to ~0.05 times those for steel tubes. For the highest velocity data point, the mass losses for the refractory metal tubes are 0.25 to 0.45 times those for steel tubes.

### D. Profiles of tube mass losses

Figure 9 shows the CFD profiles along the gun for tube mass losses for steel, rhenium and tantalum tubes for conditions of shot 33-93. This shot is identified in Figs. 6 – 8. Figure 10 shows the corresponding data for shot 20-80 and Fig. 11 shows the corresponding data for shot 18-78. These shots are also identified in Figs. 6 – 8. The data for shot 18-78 are reasonably representative for the remaining 6 shots modeled, except that for the 3 lowest muzzle velocity shots, there is zero erosion with rhenium tubes and two of these three shots have zero erosion with tantalum tubes. (For Figs. 9 – 11, the blind end of the powder breech is at 0.0 cm and the gun muzzle is at 2019.4 cm. “Cone start” and “cone end” refer to the contraction cone in the high pressure coupling.)

The following discussion relates to the results shown in Figs. 9 to 11 plus corresponding results for the remaining six shots modeled; the latter are not shown herein, in the interests of brevity. For steel tubes, erosion is predicted over a tube length of 165 – 280 cm, with about 45 cm of erosion up range of the diaphragm (at x = 1635 cm in Figs. 9 to 11) and the remainder downrange. With the exception of the highest velocity shot, shot 33-93, the tube lengths with erosion are very much less with the refractory metal tubes, being zero to ~40 cm for tantalum tubes and zero to ~25 cm for rhenium tubes. The maximum wall retreats for steel tubes are 0.003 – 0.005 cm for seven shots, 0.008 cm for the second fastest shot (shot 20-80) and 0.012 cm for the fastest shot (shot 33-93). For tantalum tubes, the corresponding numbers are 0.0 – 0.0023 cm (seven shots), 0.004 cm (shot 20-80) and 0.0065 cm (shot 33-93). For rhenium tubes, the corresponding numbers are 0.0 – 0.0013 cm (seven shots), 0.0028 cm (shot 20-80) and 0.0049 cm (shot 33-93).

### E. Overall picture of results, suitability of tantalum as a liner/coating material

The results of the CFD calculations shown in Figs. 7 – 11 predict that there would be somewhat more erosion for tantalum tubes than for rhenium tubes. However, with the exception of the highest velocity shot, the erosion of tantalum remains much less than that for steel tubes (see Figs. 7 and 8), and the tantalum tubes are seen to be very nearly equal in muzzle velocity performance to rhenium tubes (see Fig. 6). Even for the highest velocity shot, the tantalum tubes produce about 82% of the muzzle velocity gain over steel tubes that can be obtained with rhenium tubes.

In the discussion of Sec. IIIB, it was noted that tantalum has a lower elastic modulus than steel whereas rhenium has a higher modulus than steel. Thus, a tantalum coating will transmit the load to a backing thick steel tube much more effectively than rhenium. Tantalum also has a much greater ductility than rhenium. This will make a tantalum coating more able than rhenium to follow the thermal and pressure stresses and strains of gun firing without cracking. Further, tantalum and tantalum alloy liners/coatings have been successfully implemented in military powder guns. Overall, tantalum appears to be preferred to rhenium as a liner/coating material for two stage light gas guns to reduce tube erosion and increase muzzle velocity.

## VII. SOME PRACTICAL CONSIDERATIONS

### A. Size scaling of results

Here, we examine the question of the scaling of the results presented in Secs. IV to VI with gun size. For two reasons, these results do not scale directly with gun size. We consider two guns, one twice the size of the other. All gun operating conditions are considered to be directly scaled up with size; i.e., pressures are the same, lengths and diameters are scaled by a factor of two and masses are scaled by a factor of $2^3 = 8$. At first, we ignore Reynolds numbers effects and thus take the wall heat fluxes to be identical for the two guns. Corresponding points in the gun tube walls will reach the melting point at exactly the same time (in milliseconds) for the two guns. Since the gun cycle is twice as long for the larger gun, erosion of the tube wall take place during a larger fraction of the gun cycle for the larger gun. Second, the heat capacity of the tube wall of the larger gun is not twice that of the smaller gun, but only $\sqrt{2}$ times that of the smaller gun, since the thermal depth in the tube wall of the larger gun varies as $\sqrt{\text{time}}$, which varies as $\sqrt{\text{size}}$. Hence, a greater fraction of the heat load to the wall of the larger gun must go into erosion of the tube material. Both of these effects tend to make the erosion greater for the larger gun. On the other hand, the heat transfer tends to vary with (Reynolds number)$^{-0.2}$ in turbulent flow and, hence, the heat fluxes would be expected to be less for the larger gun. This effect obviously is in the other direction and favors the larger gun. The results presented herein for 0.5” guns thus cannot simply be scaled to other size guns; rather, a new set of numerical calculations must be made for other size guns.

### B. Other considerations - part of gun to be lined, diaphragms

In this section, based on numerical predictions and experimental measurements of gun erosion, we give suggestions for the lengths of the gun tubes of the Ames 0.5" gun which need to be lined with Re. Table 3 shows experimental and numerical data on the lengths of the gun tube upstream and downstream of the diaphragm where erosion was measured or predicted. In Table 3 "downstream erosion region" denotes the region between the diaphragm and the muzzle and "upstream erosion region" denotes the region extending from the diaphragm back towards the pump tube. The barrel length is 385 cm. The length of the barrel that one would need to line with a refractory metal obviously depends upon the gun operating condition. In general, however, one should expect to have to line a significantly greater distance along the barrel with a refractory metal than the distances shown in Table 3 where erosion of steel barrels was observed or predicted. This is because when one switches to refractory metal gun tubes, there will much less loss of working gas energy to the refractory metal tube than to the steel tube, since the tube wall temperature can be much higher. Thus, if one lines the barrel with a refractory metal only

out to exactly the location where erosion stops with all-steel tubes, the gas which flows over the up range end of the steel part of the tube will be much hotter than the gas which would pass this same location if the tubes were entirely made of steel. Thus, with tubes that are partly a refractory metal and partly steel, the erosion of the steel could occur at distances further down the tube than for the case of all-steel tubes. The current version of the code does not allow the modeling of gun tubes that are partly a refractory metal and partly steel. We make a rough estimate that the refractory metal liner must extend 20% of the barrel length (or 77 cm) beyond the location where erosion stops with all-steel barrels in order to minimize tube erosion. In this case, anywhere from 200 to 312 cm of the tube must be lined with a refractory metal to minimize erosion and hydrogen loading.

**Table 3. Lengths of gun tube where erosion was observed or predicted**

| Number of shots | Reference number | Figure number | L, downstream erosion region (cm) | L, upstream erosion region (cm) |
|---|---|---|---|---|
| 9 | present work | 9 - 11 | 123 - 235 | 41 - 48 |
| 40 | 3 | 5 | 110[E] | No data |
| 118 | 11 | 9 | No data | 35[E] |

[E]experimental results

It appears from the table that the part of the gun extending up range from the diaphragm (towards the conical high pressure coupling) need only be lined for a length of about 45 cm to minimize erosion of the gun bore. Since the flow is toward, rather than away, from the region of the refractory metal liner, there is no need to extend the region with the refractory metal liner beyond the erosion distance shown in the table.

Our final point here is to mention diaphragm erosion. In the numerical calculations, the diaphragm does not exist as a solid body that can be heated and eroded. One simply has a boundary condition which one changes when the diaphragm ruptures. Hence, there is no allowance for diaphragm erosion. Since the code predicts the experimental muzzle velocities of shots fired with steel gun tubes rather well (Figs. 2 and 5), one does not expect that a large fraction of the eroded material loading down the hydrogen comes from the diaphragm. However, it is quite possible that 10 - 15% of the material loading down the hydrogen comes from the diaphragm. We would not be able to distinguish such a small fraction from the degree of agreement between the experimental and numerical muzzle velocity data of Figs. 2 and 5. If one lines the regions of the gun tube suggested in the previous paragraphs with a refractory metal and erosion of the tubes proper is minimized, the material eroded from the diaphragm may become significant in limiting the muzzle velocity. In this case, one may want to consider diaphragms coated with a refractory metal.

12

## VIII. SUMMARY AND CONCLUSIONS

Two stage light gas guns with steel gun tubes were modeled in earlier studies[3,12]. These studies gave good predictions of muzzle velocities and gun erosion for 45 shots, which had been made with the Ames 0.5" light gas gun. A large number (36) of these shots were then remodeled, assuming the tube wall material eroded at each time step vanished before being incorporated into the hydrogen working gas. In

these calculations, the hydrogen working gas was not loaded down with eroded gun tube material and large (2 - 4 km/sec) increases in muzzle velocity were predicted. It was then decided to see what fraction of these large muzzle velocity increases would remain if the calculations included loading down of the working gas with eroded gun tube material, and the gun tube material was changed from steel to a refractory metal.

In the studies of Ref. 10, rhenium was chosen as the refractory metal gun tube material. Seventeen of the highest performance steel gun tube shots were remodeled with rhenium gun tubes. Sixteen of these numerical calculations showed zero erosion of the rhenium tubes by the hydrogen gas and continued to show the aforementioned large increases in muzzle velocity. Since these calculations are realistic, these muzzle velocity increases are predicted to be realizable in practice using Re gun tubes. For an erosive shot, profiles of maximum tube wall temperature, hydrogen mass fraction, density and pressure were shown in Ref. 10 for a shot with steel tubes and the corresponding shot with rhenium tubes. A consistent picture of tube wall material erosion, weighing down of the hydrogen working gas with wall material and projectile drive pressure loss due to acceleration of eroded wall material incorporated into the working gas was shown for steel tubes but not for rhenium tubes.

The nine high performance shots modeled for rhenium tubes with the older version of the code in Ref. 10 and shown in Fig. 3, were then remodeled with the new version of the code for steel, tantalum and rhenium gun tubes. Muzzle velocities for the three types of gun tube material were presented. It was shown that, with the exception of the highest velocity shot, the muzzle velocity gains with tantalum tubes (when compared with steel tubes) are very nearly the same as those achievable with rhenium tubes. Even for the highest velocity shot, the tantalum/steel velocity gain is 82% that of the rhenium/steel velocity gain. Correlations of total gun tube mass loss and profiles of tube wall retreat and mass loss along the gun tube were presented and discussed. For all except one shot, tube mass losses for rhenium and tantalum tubes were 0 – 5% and 0 – 14%, respectively, of those for steel tubes.

Tantalum has a lower elastic modulus than steel whereas rhenium has a higher modulus than steel. Thus, a tantalum coating will transmit the load to a thick steel backup tube much more effectively than a rhenium coating. Tantalum also has a much greater ductility than rhenium and hence, will better be able to follow the thermal and pressure stresses and strains of gun firing without cracking. Finally, tantalum and tantalum alloy liners/coatings have been successfully implemented in military powder guns. Overall, tantalum appears to be preferred over rhenium as the liner/coating material for two stage light gas guns to reduce tube erosion and increase muzzle velocity.

Scaling of the numerical results to guns of different sizes was discussed. A simple, direct scaling is incorrect; rather, the full calculations would need to be repeated for guns of different sizes. Based on numerical and experimental results, estimates are given for the length of the gun tubes on both sides of the diaphragm that need to be lined with refractory metal to minimize erosion of the tubes. The possible use of a diaphragm coated with a refractory metal was also discussed.

## ACKNOWLEDGEMENT

Support by NASA (Contract NNA15BB15C) to Analytical Mechanics Associates, Inc. is gratefully acknowledged.

## REFERENCES

1. Canning, T. N., Seiff, A. and James, C. S., “Ballistic Range Technology,” AGARDOgraph 138, August, 1970, pp. 11 - 95.

2. Ebihara, W. T. and Rorabaugh, D. T., "Mechanisms of Gun-Tube Erosion and Wear," in *Gun Propulsion Technology*, edited by Stiefel, L., Vol. 109, Progress in Aeronautics and Astronautics, AIAA, Washington, 1988, pp. 357-376.
3. Bogdanoff, D. W., "CFD Modelling of Bore Erosion in Two-Stage Light Gas Guns," presented at the 49th Aeroballistic Range Association Meeting, Scheveneingen, the Netherlands, October 5 - 9, 1998.
4. Canning, T. N., Seiff, A. and James, C. S., "Ballistic Range Technology," op. cit., pp. 41 - 44.
5. Chavez, D. J., King, C. C. and Linley, L. L., "A Study to Optimize a 7.6-mm (30-caliber) Two-Stage Light Gas Gun," presented at the 42nd Aeroballistic Range Association Meeting, Adelaide, South Australia, October 21-25, 1991.
6. DeWitt, J. R., "Configuration Development of the New AEDC 3.3 Inch Launcher," presented at the 45th Aeroballistic Range Association Meeting, University of Alabama at Huntsville, Huntsville, Alabama, October 10-14, 1994.
7. Bogdanoff, D. W. and Miller, R. J., "Optimization Study of the Ames 1.5" Two-Stage Light Gas Gun," AIAA paper 96-0099, presented at the 34th AIAA Aerospace Sciences Meeting, Reno, NV, January 15-18, 1996.
8. Bogdanoff, D. W. and Miller, R. J., "Recent Developments in Gun Operating Techniques at the NASA Ames Ballistic Ranges," NASA TM 110387, March, 1996.
9. Bogdanoff, D. W., "Optimization Study of the Ames 0.5" Two-Stage Light Gas Gun," NASA TM 110386, March, 1996.
10. Bogdanoff, D. W., "Use of a Rhenium Liner to Reduce Bore Erosion in Two-Stage Light Gas Guns," presented at the 50th Aeroballistic Range Association Meeting, Pleasanton, California, November 8 - 12, 1999.
11. Bogdanoff, D. W. and Miller, R. J., "New Higher-Order Godunov Code for Modelling Performance of Two-Stage Light Gas Guns", NASA TM 110363, September, 1995.
12. Bogdanoff, "CFD Modelling of Bore Erosion in Two-Stage Light Gas Guns," NASA TM 112236, August, 1998.
13. Knuth, E. L. and Dershin, H., "Use of Reference States in Predicting Transport Rates in High-Speed Turbulent Flows with Mass Transfer," *International Journal of Heat and Mass Transfer*, Vol. 6, 1963, pp. 999-1018.
14. Bogdanoff, D. W., "Ram Accelerator Direct Space Launch System: New Concepts," *Journal of Propulsion and Power*, Vol. 8, March-April, 1992, pp. 488-489 (Appendix C).
15. Tauber, M. E., "A Review of High-Speed Convective Heating Computational Methods," NASA Technical Paper 2914, July 1989, p. 19.
16. Jeromin, L. O. F., "The Status of Research in Turbulent Boundary Layers with Fluid Injection," *Progress in Aeronautical Sciences*, Vol. 10, 1970, pp. 153-162.
17. Steifel, L., ed., "Gun Propulsion Technology," Vol. 109, Progress in Astronautics and Aeronautics series, published by the American Institute of Aeronautics and Astronautics, 1988, p. 315.
18. *Machine Design*, December 1993, pp. 33, 90, 91.
19. Holman, J. P., "Heat Transfer," 6th ed., McGraw-Hill, New York, 1986, p. 635.
20. Steifel, L., ed., op. cit., p. 339-340.
21. ibid, pp. 338-339.
22. ibid, pp. 347.
23. Ahmad, I., Barranco, J., Aalto, P. and Cox, J., "Studies of Refractory Metal Coatings for Advanced Gun Barrels," US Army Armament Research and Development Center, Benet

Weapons Laboratory, Watervliet, NY, Technical Report ARLCB-TR-83029, July, 1983, especially pp. 40-47.
24. Cullinan, R., D'Andrea, G., Croteau, P. and Arnold, C., "Study of Erosion Resistant Materials for Gun Tubes: Part I, 20 mm Technology," US Army Armament Research and Development Center, Benet Weapons Laboratory, Watervliet, NY, Technical Report ARLCB-TR-80027, December 1980, especially pp. 96-97 (summary).
25. Ho, C. Y., Powell, R. W. and Liley, P. E., "Thermal Conductivity of the Elements, A Comprehensive Review," *Journal of Physical and Chemical Reference Data*, Vol. 3, 1974, Supplement No. 1, pp. 548 - 552.
26. Touloukian, Y. S. and Buyco, E. H., "Specific Heat; Metallic Elements and Alloys," Plenum, New York, 1970, pp. 181 - 183.
27. Touloukian, Y. S., Kirby, R. K., Taylor, R. E. and Desai, P. D., "Thermal Expansion, Metallic Elements and Alloys," Vol. 12 in the series *Thermophysical Properties of Matter*, Plenum, New York, 1975, pp. 280 - 284.
28. R. C. Weast and Astle, M. J., "CRC Handbook of Chemistry and Physics," 61st ed., CRC Press, Boca Raton, Florida, 1980, pp. B253 - B257.
29. ibid., pp. B2 - B48.
30. Washburn, E. W., editor-in-chief, "International Critical Tables of Numerical Data, Physics, Chemistry and Technology," McGraw-Hill, New York, 1926, Vol. II, p. 46.
31. Ho, C. Y., Powell, R. W. and Liley, P. E., op, cit., p. 631.
32. Touloukian, Y. S. and Buyco, E. H., op. cit., pp. 221 - 228.
33. Lampman, S. R. and Zorc, T. B., technical editors, Metals Handbook, 10th ed., Vol 2. Properties and Selection: Nonferrous Alloys and Special-Purpose Materials, ASM International, October, 1990, p. 1161.
34. Touloukian, Y. S., Kirby, R. K., Taylor, R. E. and Desai, P. D, op. cit., pp. 316 - 317.
35. Website periodictable.com.
36. Paradis, P.-F., Ishikawa, T. and Yoda. S., "Noncontact Density Measurements of Tantalum and Rhenium in the Liquid and Undercooled States," *Applied Physics Letters*, Vol. 83, No. 19, 10 November, 2003, pp. 4047 – 4049.
37. Bogdanoff, D. W. and Miller R. J., "Improving the Performance of Two-Stage Light Gas Guns by Adding a Diaphragm in the Pump Tube," *Int. J. Impact Engng*, Vol. 17, 1995, pp. 81 – 92.
38. Canning, T. N., Seiff, A. and James, C. S., "Ballistic Range Technology," op. cit., p. 58.

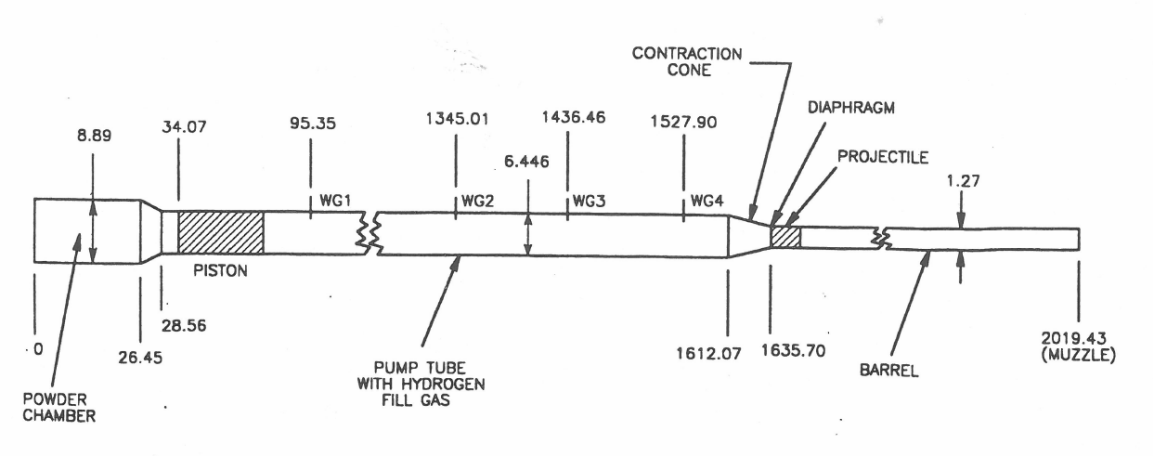


Fig. 1. Schematic sketch of Ames 0.5” light gas gun. Numbers (in cm) are bore diameters or distances from the blind end of the powder chamber. WG1 – WG4 denote whisker gauges for the measurement of piston velocity.

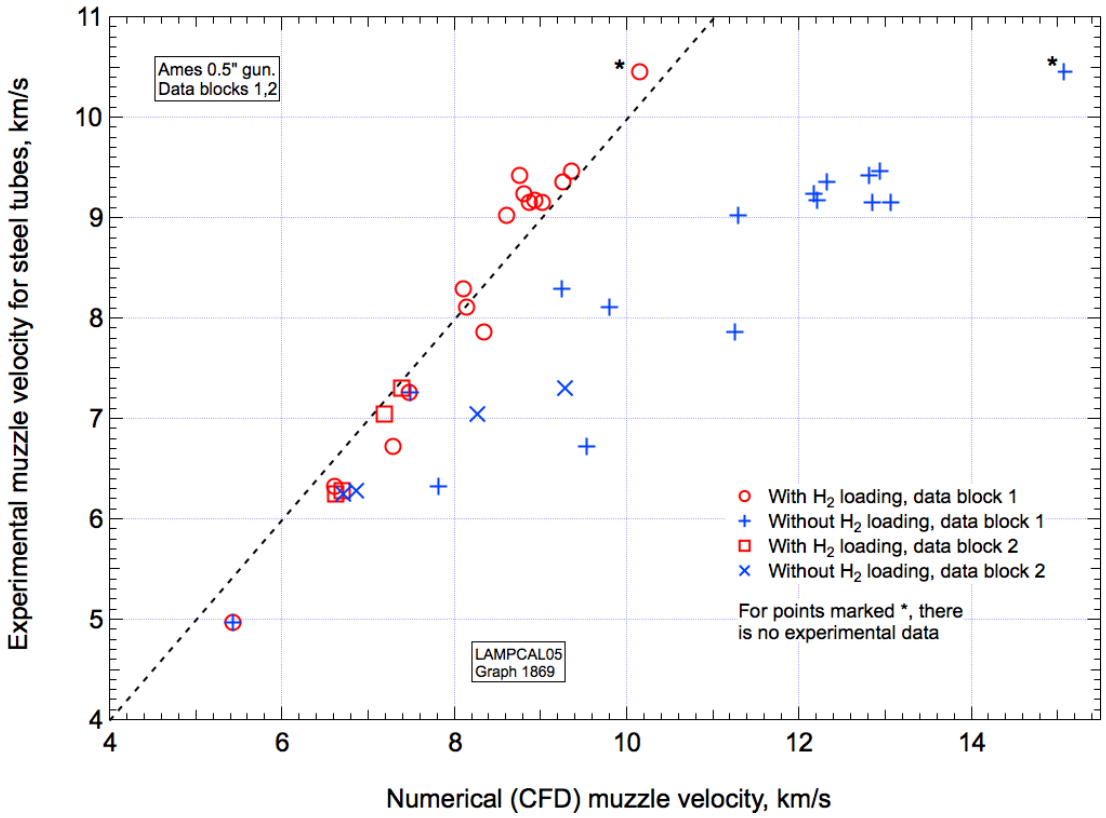


16

Fig. 2. Experimental and numerical muzzle velocities for Ames 0.5” gun for data blocks 1 and 2. Steel gun tubes.

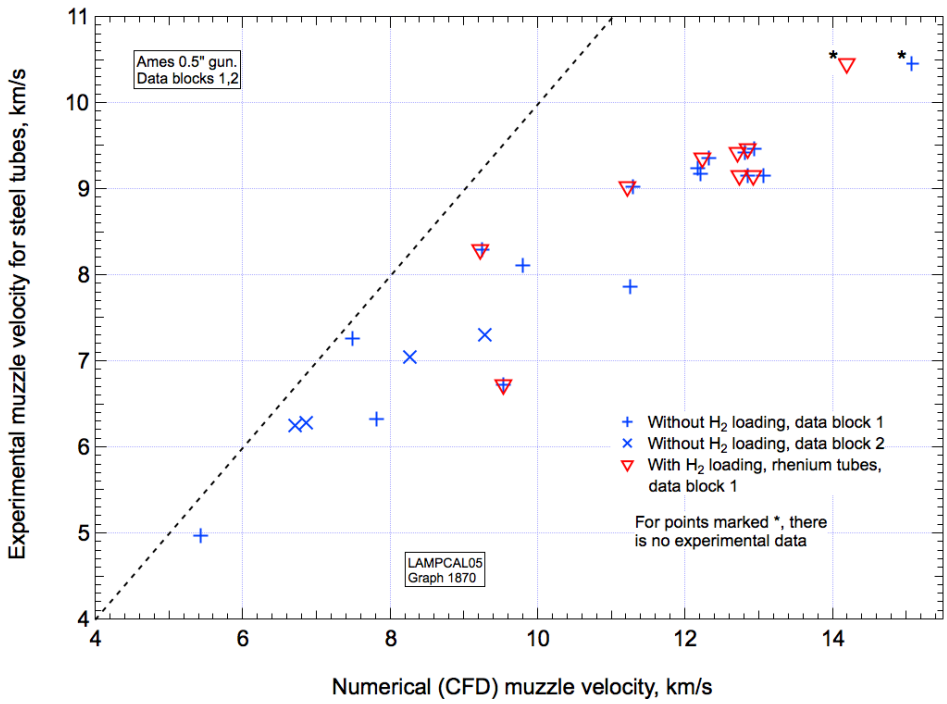


Fig. 3. Numerical (CFD) muzzle velocities for Ames 0.5" gun for data blocks 1 and 2 plotted versus experimental muzzle velocities for steel tubes. Numerical muzzle velocities for steel tubes have no hydrogen loading, while numerical muzzle velocities for rhenium tubes do have hydrogen loading.

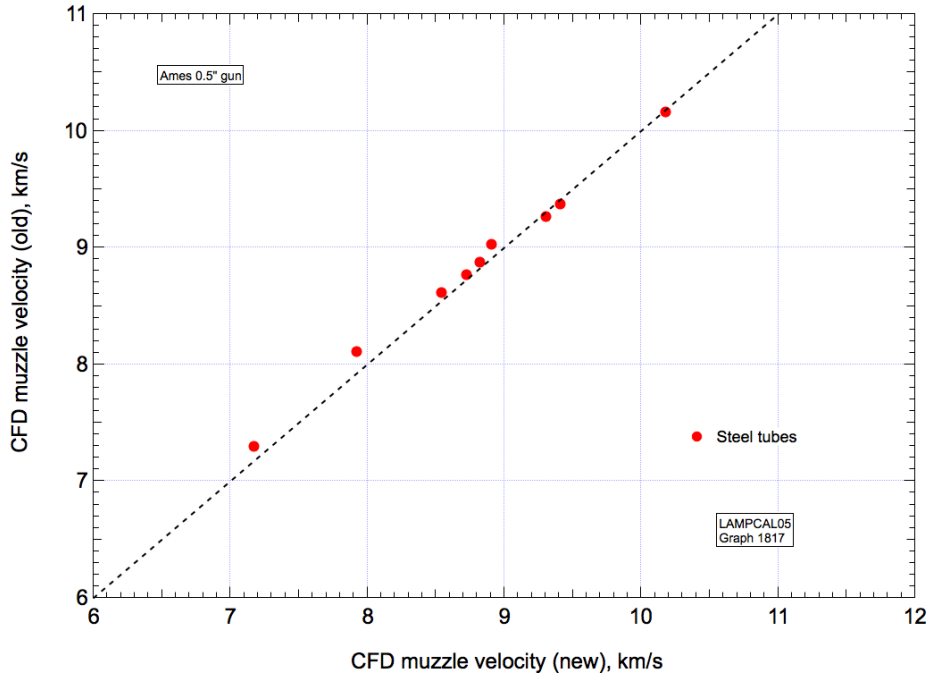


Fig. 4. Numerical (CFD) muzzle velocities for Ames 0.5" gun for steel tubes with hydrogen loading for nine high performance shots of data block 1. Values for the older version of the code and the current version are compared.

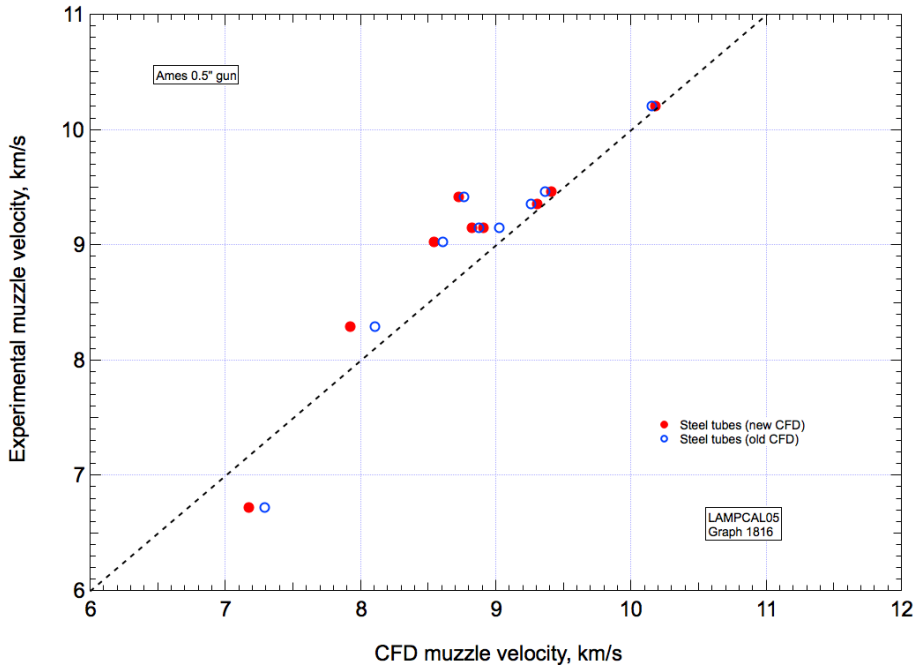


Fig. 5. Experimental and numerical (CFD) muzzle velocities for Ames 0.5" gun for steel tubes with hydrogen loading for nine high performance shots of data block 1. Numerical values for both the older and the current versions of the code are shown.

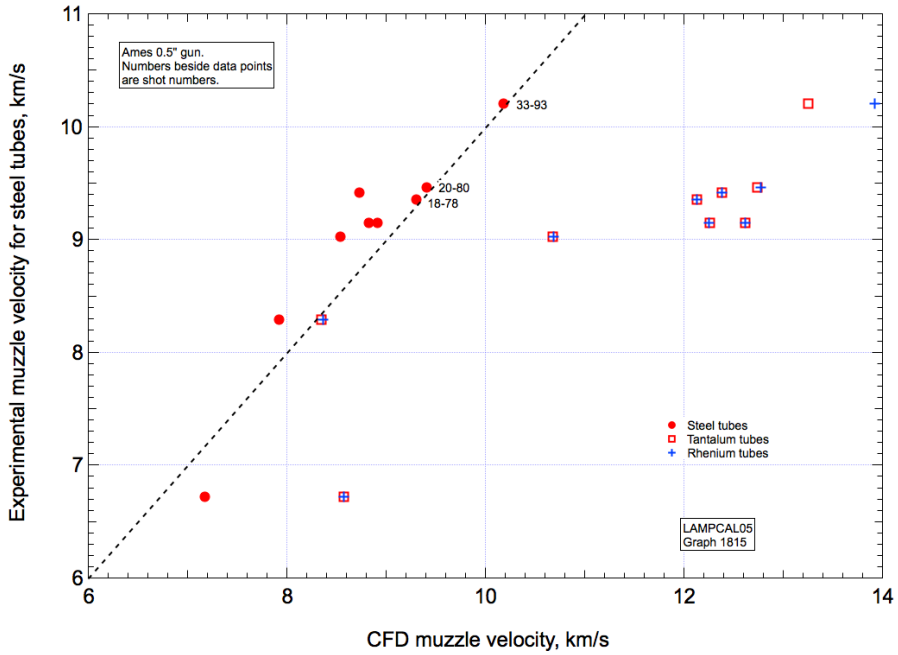


Fig. 6. CFD muzzle velocities for Ames 0.5" gun for steel, Ta and Re tubes with hydrogen loading for nine high performance shots of data block 1 plotted versus experimental muzzle velocities for steel tubes. All CFD values calculated with the current version of the code.

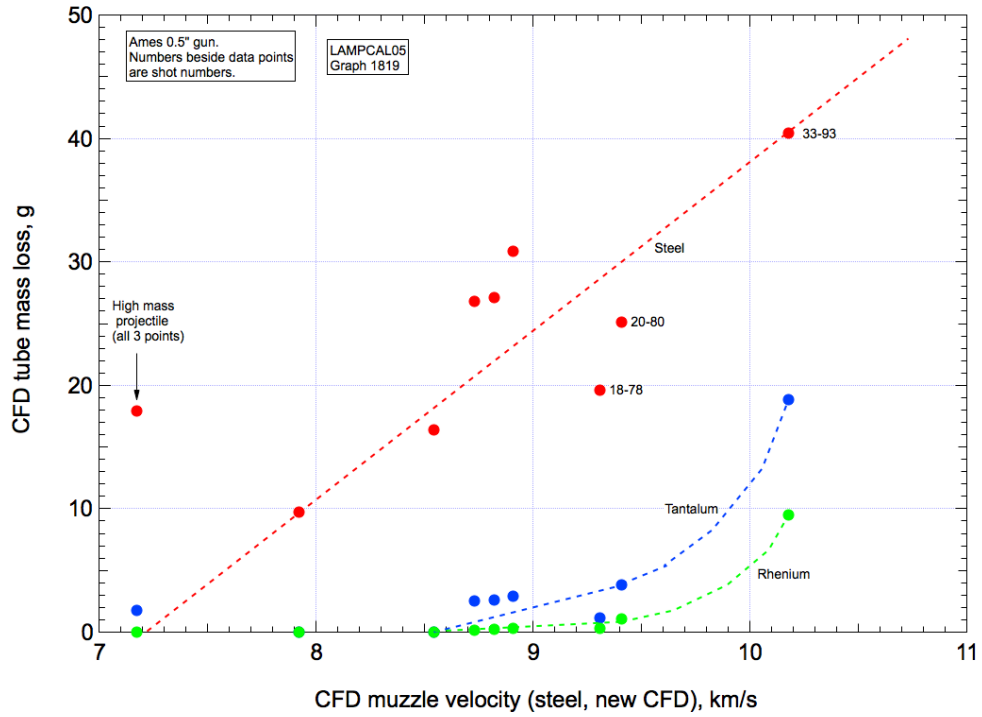


Fig. 7. CFD tube mass losses for Ames 0.5” gun for steel, Ta and Re tubes plotted versus CFD muzzle velocities for steel tubes.

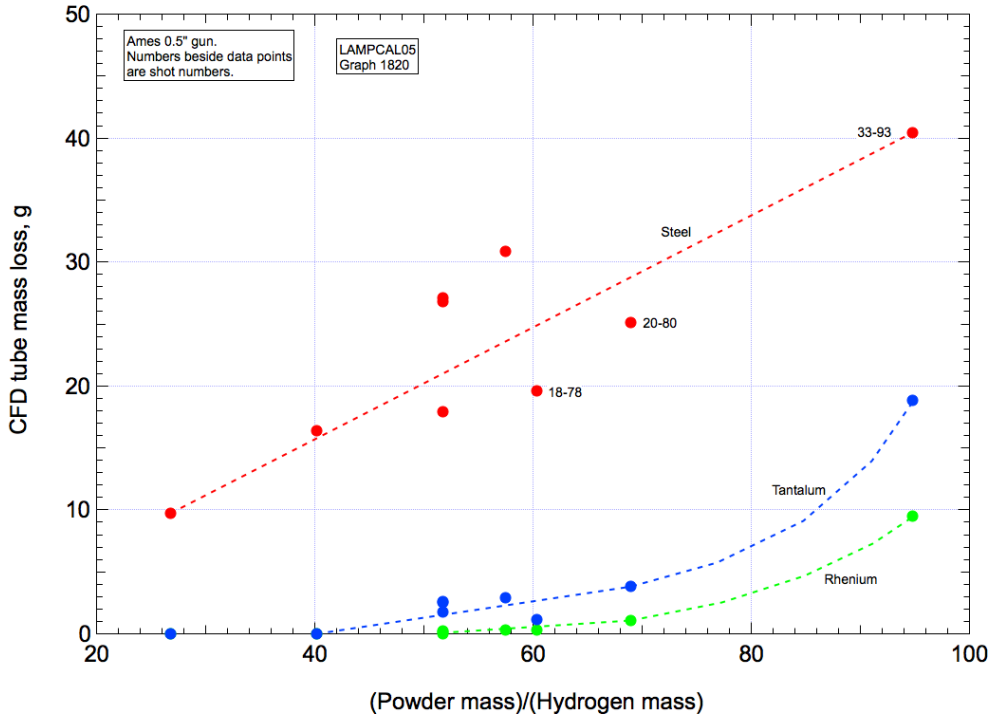


Fig. 8. CFD tube mass losses for Ames 0.5” gun for steel, Ta and Re tubes plotted versus the ratio of powder mass to hydrogen mass.

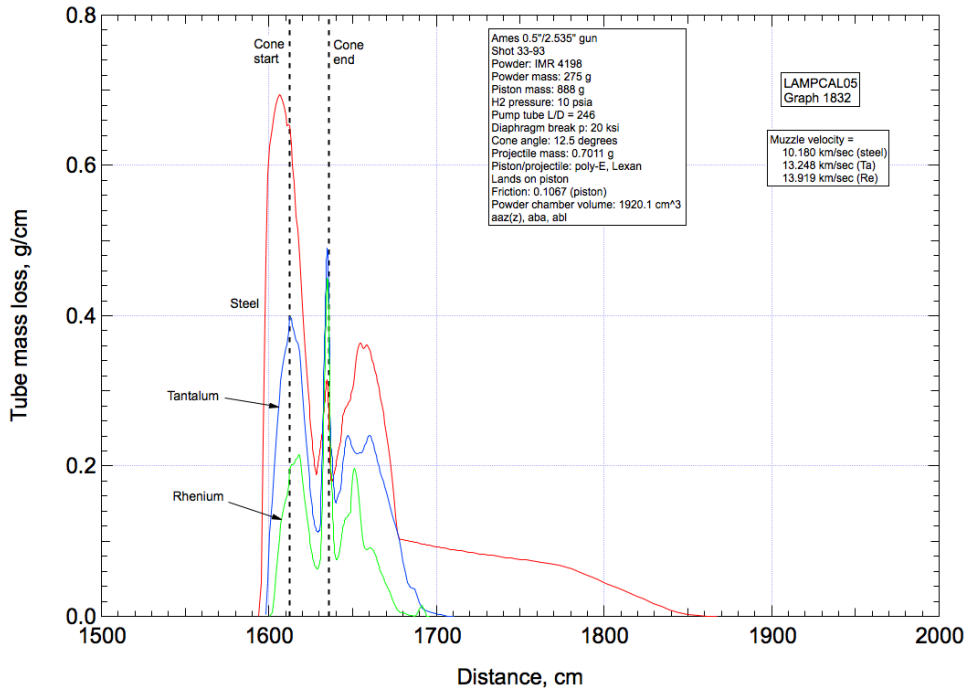


Fig. 9. CFD tube mass losses for shot 33-93 for Ames 0.5" gun for steel, Ta and Re tubes plotted versus distance along gun.

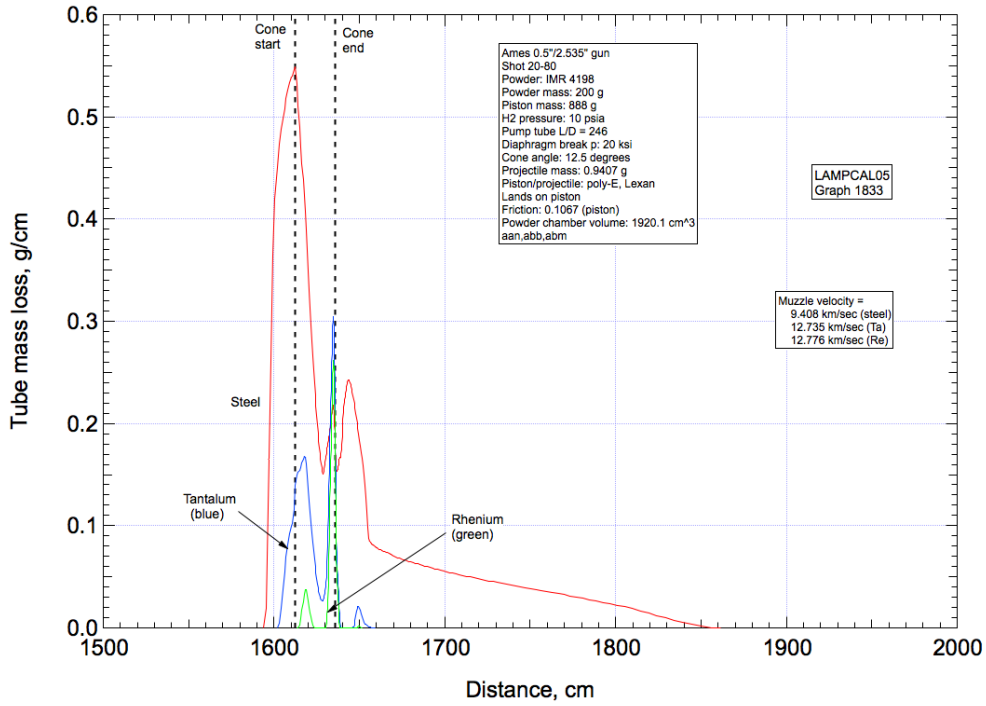


Fig. 10. CFD tube mass losses for shot 20-80 for Ames 0.5" gun for steel, Ta and Re tubes plotted versus distance along gun.

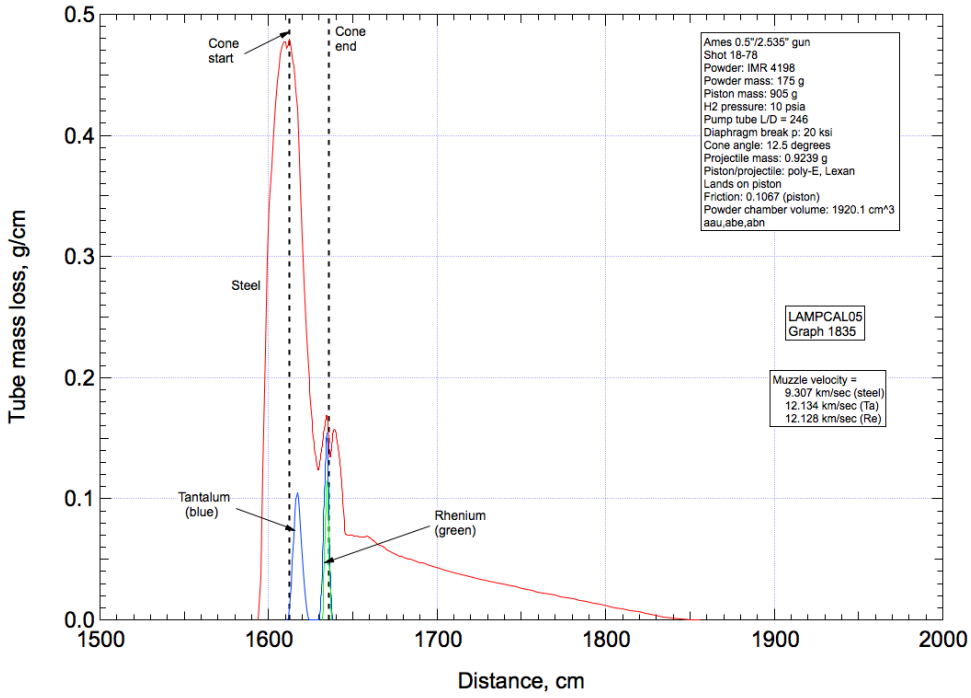


Fig. 11. CFD tube mass losses for shot 18-78 for Ames 0.5" gun for steel, Ta and Re tubes plotted versus distance along gun.